Evolutionarily conserved *Tbx5–Wnt2/2b* pathway orchestrates cardiopulmonary development

Jeffrey D. Steimle[a,b,c], Scott A. Rankin[d,e,f,g], Christopher E. Slagle[h,i,j,k], Jenna Bekeny[a,b,c], Ariel B. Rydeen[a,b,c], Sunny Sun-Kin Chan[l,m], Junghun Kweon[a,b,c], Xinan H. Yang[a,b,c], Kohta Ikegami[a,b,c], Rangarajan D. Nadadur[a,b,c], Megan Rowton[a,b,c], Andrew D. Hoffmann[a,b,c], Sonja Lazarevic[a,b,c], William Thomas[n,o], Erin A. T. Boyle Anderson[p], Marko E. Horb[n,o], Luis Luna-Zurita[q,r], Robert K. Ho[m], Michael Kyba[l,m], Bjarke Jensen[s], Aaron M. Zorn[d,e,f,g], Frank L. Conlon[h,i,j,k], and Ivan P. Moskowitz[a,b,c,1]

[a]Department of Pediatrics, University of Chicago, Chicago, IL 60637; [b]Department of Pathology, University of Chicago, Chicago, IL 60637; [c]Department of Human Genetics, University of Chicago, Chicago, IL 60637; [d]Center for Stem Cell and Organoid Medicine, Cincinnati Children's Research Foundation, Cincinnati, OH 45229; [e]Department of Pediatrics, College of Medicine, University of Cincinnati, Cincinnati, OH 45229; [f]Division of Developmental Biology, Perinatal Institute, Cincinnati Children's Research Foundation, Cincinnati Children's Hospital Medical Center, University of Cincinnati, Cincinnati, OH 45229; [g]Department of Pediatrics, College of Medicine, University of Cincinnati, Cincinnati, OH 45229; [h]Department of Biology, University of North Carolina at Chapel Hill, Chapel Hill, NC 27599; [i]Department of Genetics, University of North Carolina at Chapel Hill, Chapel Hill, NC 27599; [j]Integrative Program for Biological and Genome Sciences, University of North Carolina at Chapel Hill, Chapel Hill, NC 27599; [k]The University of North Carolina McAllister Heart Institute, University of North Carolina at Chapel Hill, Chapel Hill, NC 27599; [l]Department of Pediatrics, University of Minnesota, Minneapolis, MN 55455; [m]Lillehei Heart Institute, University of Minnesota, Minneapolis, MN 55455; [n]National Xenopus Resource, Marine Biological Laboratory, Woods Hole, MA 02543; [o]Eugene Bell Center for Regenerative Biology and Tissue Engineering, Marine Biological Laboratory, Woods Hole, MA 02543; [p]Department of Organismal Biology and Anatomy, University of Chicago, Chicago, IL 60637; [q]Gladstone Institute of Cardiovascular Disease, San Francisco, CA 94158; [r]Roddenberry Center for Stem Cell Biology and Medicine, Gladstone Institutes, San Francisco, CA 94158; and [s]Amsterdam Cardiovascular Sciences, Department of Medical Biology, Amsterdam University Medical Center, University of Amsterdam, 1105AZ Amsterdam, The Netherlands

Edited by Roeland Nusse, Stanford University School of Medicine, Stanford, CA, and approved September 27, 2018 (received for review July 9, 2018)

Codevelopment of the lungs and heart underlies key evolutionary innovations in the transition to terrestrial life. Cardiac specializations that support pulmonary circulation, including the atrial septum, are generated by second heart field (SHF) cardiopulmonary progenitors (CPPs). It has been presumed that transcription factors required in the SHF for cardiac septation, e.g., *Tbx5*, directly drive a cardiac morphogenesis gene-regulatory network. Here, we report instead that TBX5 directly drives Wnt ligands to initiate a bidirectional signaling loop between cardiopulmonary mesoderm and the foregut endoderm for endodermal pulmonary specification and, subsequently, atrial septation. We show that *Tbx5* is required for pulmonary specification in mice and amphibians but not for swim bladder development in zebrafish. TBX5 is non–cell-autonomously required for pulmonary endoderm specification by directly driving *Wnt2* and *Wnt2b* expression in cardiopulmonary mesoderm. TBX5 ChIP-sequencing identified *cis*-regulatory elements at *Wnt2* sufficient for endogenous *Wnt2* expression domains in vivo and required for *Wnt2* expression in precardiac mesoderm in vitro. *Tbx5* cooperated with Shh signaling to drive *Wnt2b* expression for lung morphogenesis. *Tbx5* haploinsufficiency in mice, a model of Holt–Oram syndrome, caused a quantitative decrement of mesodermal-to-endodermal Wnt signaling and subsequent endodermal-to-mesodermal Shh signaling required for cardiac morphogenesis. Thus, *Tbx5* initiates a mesoderm–endoderm–mesoderm signaling loop in lunged vertebrates that provides a molecular basis for the coevolution of pulmonary and cardiac structures required for terrestrial life.

lung development | heart development | TBX5 | Wnt signaling | Hedgehog signaling

Utilization of atmospheric oxygen revolutionized the ability of vertebrates to adapt to terrestrial life (1). At the center of this revolution are the lungs, a foregut-derived gas-exchange structure (1, 2). The derived cardiovascular system, utilizing pulmonary oxygen, must manage blood from both the body and the lungs simultaneously (2). While most lungfish, amphibians, and reptiles exhibit a three-chambered heart with an atrial septum separating pulmonary and systemic circulation entering the heart (3), the two-sided, four-chambered crocodilian, avian, and mammalian hearts have independently evolved to completely separate pulmonary from systemic circulation (4). The proper development and placement of the cardiac septa are critical for the efficient handling of blood, and defects in these structures comprise common forms of human congenital heart disease.

Recent work has highlighted the common developmental origin of multiple mesodermal derivatives in both the heart and the lung (5, 6). This lateral plate mesodermal population has been termed the "second heart field" (SHF) or "cardiopulmonary progenitors" (CPPs). This population originates dorsal to the cardiac inflow tract and ventral to the anterior foregut and generates multiple structures in the heart, e.g., the atrial septum, and in the lungs, e.g., smooth muscle and vascular endothelium (5, 6). This essential CPP region is labeled by expression of the canonical Wnt signaling ligand *Wnt2*, the Hedgehog (Hh)

Significance

In the 20 years since the discovery of the genetic link between the transcription factor *TBX5* and congenital heart defects, few direct targets of *TBX5* in cardiac morphogenesis have been identified. In this work, we demonstrate that TBX5 directly regulates canonical Wnt ligands required for initiation of lung development. Lung endoderm forms a Hedgehog signaling source required for morphogenesis of both the lungs and the cardiac inflow septum. Our work expands the role of TBX5 to include a non–cell-autonomous component for atrial septation. We find the mesoderm–endoderm–mesoderm signaling loop initiated by TBX5 is evolutionarily conserved from amphibians to mammals. This work suggests that the evolutionary origin of lungs may have involved the recruitment of cardiac TBX5.

Author contributions: J.D.S., S.A.R., C.E.S., E.A.T.B.A., M.E.H., R.K.H., B.J., A.M.Z., F.L.C., and I.P.M. designed research; J.D.S., S.A.R., C.E.S., J.B., A.B.R., J.K., K.I., R.D.N., M.R., A.D.H., S.L., W.T., E.A.T.B.A., L.L.-Z., and B.J. performed research; S.S.-K.C. and M.K. contributed new reagents/analytic tools; J.D.S., S.A.R., C.E.S., and X.H.Y. analyzed data; and J.D.S., S.A.R., A.M.Z., F.L.C., and I.P.M. wrote the paper.

The authors declare no conflict of interest.

This article is a PNAS Direct Submission.

Data deposition: RNA-sequencing, ChIP-sequencing, and ATAC-sequencing data have been deposited in the Gene Expression Omnibus databank (accession nos. GSE75077 and GSE119885).

[1]To whom correspondence should be addressed. Email: imoskowitz@uchicago.edu.

This article contains supporting information online at www.pnas.org/lookup/suppl/doi:10.1073/pnas.1811624115/-/DCSupplemental.

Published online October 23, 2018.

signaling-responsive transcription factor *Gli1*, and the T-box family transcription factor *Tbx5* (5, 7–9).

Mutations in *TBX5* have been implicated as the primary genetic cause of Holt–Oram syndrome (HOS), a human syndrome that includes cardiac septal defects (10–14). Previous work has demonstrated that *Tbx5* is required in the posterior SHF (pSHF) for atrial septation (7, 9, 15). In addition, Sonic hedgehog (Shh) signaling has been implicated in cardiac septation (7–9, 16). *Shh*, expressed in the pulmonary endoderm (PE), activates GLI-mediated transcription in the CPPs (7, 8). *Shh* and *Tbx5* genetically interact for cardiac septation, and constitutive activation of Hh signaling in CPPs rescues atrial septal defects caused by reduced *Tbx5* dose (7, 9). Furthermore, TBX5 and GLI transcription factors directly cooperate at enhancers for genes required for cardiac septation (7, 9). This has generated a model in which TBX5 and GLI transcription factors directly activate gene expression in the CPPs of the pSHF for cardiac morphogenesis.

CPPs are an important source of signals that induce the pulmonary lineage in the ventral foregut endoderm and contribute directly to the atrial septum and cardiopulmonary vasculature (17–19). An evolutionarily conserved paracrine signaling cascade involving retinoic acid, Hh, Wnt signaling, and bone morphogenic protein (BMP) regulates the induction of pulmonary progenitors from amphibians to mammals (5, 17–21). *Tbx5* has been implicated in lung morphogenesis, both alone and in combination with *Tbx4* (22). Midgestation conditional deletion of *Tbx5* in mouse embryos caused deficiency in lung-branching morphogenesis, and combined deletion of *Tbx4* and *Tbx5* in allelic combinations caused reduced WNT2 and BMP4 signaling (22).

We report that *Tbx5* is required non–cell-autonomously for the initiation of PE and lung formation. We find that *Tbx5* is required for the initiation of lung development in both mammals and amphibians but not for the swim bladder (SB) in zebrafish. Furthermore, we show that TBX5 directly drives the lung-inducing ligands *Wnt2* and *Wnt2b* in pSHF CPPs. TBX5-driven mesoderm-to-endoderm canonical Wnt signaling is required for the subsequent endoderm-to-mesoderm Shh signaling required for atrial septation. *Tbx5* haploinsufficiency diminishes both mesodermal *Wnt2* and endodermal *Shh* expression, suggesting that atrial septal defects in HOS may be caused in part by diminished Shh signaling rather than solely by a deficiency of a *Tbx5*-driven cell-autonomous SHF gene-regulatory network (GRN). *Tbx5* thereby initiates a mesoderm–endoderm–mesoderm signaling loop, providing a molecular basis for the coevolution of pulmonary and cardiac development.

Results

***Tbx5*-Dependent Transcriptional Profiling of the CPPs.** To investigate the role of *Tbx5* in CPPs, we performed RNA sequencing (RNA-seq) on microdissected tissue containing the CPPs from $Tbx5^{+/+}$ and $Tbx5^{-/-}$ mouse embryos at E9.5 (Fig. 1 *A* and *B*) (7, 23, 24). Compared with $Tbx5^{+/+}$ CPPs, 5,486 genes were significantly dysregulated in $Tbx5^{-/-}$ CPPs [false-discovery rate (FDR) <0.05]. We restricted our consideration of genes to those with a magnitude fold change ≥1.5 (*SI Appendix*, Table S1). This group contained 1,480 down-regulated genes and 1,588 up-regulated genes in the absence of *Tbx5* (Fig. 1*C*). The most significantly down-regulated genes in $Tbx5^{-/-}$ CPPs were transcription factors and signaling factors critical for early lung development. Notably, expression of *Nkx2-1* and the long noncoding RNA *E030019B13Rik* or NANCI, the first markers of PE specification, was extinguished (17, 25–28). Members of the Wnt and Shh signaling pathways, both required for early lung specification and morphogenesis, were also severely down-regulated (Fig. 1*C*). In addition, we observed 14 other genes among the down-regulated list that have been reported in the literature to be critical for lung development (6, 29–31). As an early role for *Tbx5* in lung development has been suggested (22, 32), we validated the significant down-regulation of 15 of 16 "lung development" genes by qRT-PCR in independent samples (Fig. 1*D*). Together, these data suggested that *Tbx5* might occupy a critical position in the GRN for lung induction.

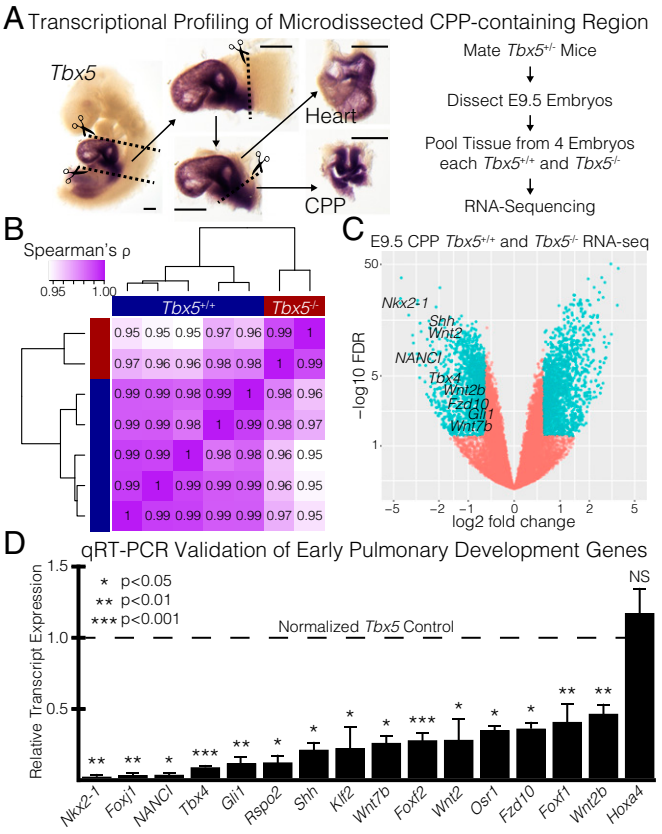

Fig. 1. Transcriptional profiling of microdissected CPPs identifies a critical role for *Tbx5* in pulmonary specification and lung development. (*A*, *Left*) Demonstration of microdissection methodology used for embryonic mouse experiments on an E9.5 embryo probed for *Tbx5* RNA by ISH. (Scale bars: 0.25 mm.) (*Right*) Transcriptional profiling strategy used to measure the *Tbx5*-dependent transcriptome in the CPP-containing tissue by RNA-seq. (*B*) Spearman's correlation of RNA-seq replicates. (*C*) Volcano plot of transcriptional profiling results with significantly dysregulated genes (teal) from the comparison of $Tbx5^{+/+}$ and $Tbx5^{-/-}$ CPPs. Early markers of the PE and canonical Wnt and Shh signaling are identified. (*D*) qRT-PCR validation of 16 early lung-development genes that were significantly dysregulated in the RNA-seq.

***Tbx5*-Dependent Lung Development Is Evolutionarily Conserved.** Utilizing the $Tbx5^{-/-}$ mouse embryos, we examined the requirement of *Tbx5* for PE specification. The earliest sign of pulmonary induction, *Nkx2-1* expression, was absent from the foregut endoderm at E9.5 by in situ hybridization (ISH) (Fig. 2*A*). Based on sagittal and coronal sections at E10.5, $Tbx5^{-/-}$ mice failed to demonstrate the earliest physical manifestation of lung morphogenesis, the outpouching of the foregut endoderm or lung buds (Fig. 2*B*). 3D reconstructions highlighting the endoderm further demonstrated the absence of lung bud initiation from the foregut in $Tbx5^{-/-}$ embryos (Fig. 2*B*).

Because of the fundamental role for *Tbx5* in lung development in mice, we asked whether this role is conserved across lunged vertebrates. Previously, an evolutionary link across amniotes has been made between *Tbx5* expression pattern in the heart and ventricular septation for efficient handling of blood (33). We first examined expression of *Tbx5* by ISH in representative species of amphibians (*Xenopus laevis*), lizards (*Anolis sagrei*), crocodilians (*Alligator mississippiensis*), and birds (*Gallus gallus*). The expression domains of *Tbx5* are conserved across each of these species with expression found in the mesodermal derivatives of the lungs in each (Fig. 2*C*).

We hypothesized that *Tbx5* may be an evolutionarily ancient driver of lung specification. We examined whether the role of *Tbx5* in lung specification was evolutionarily conserved in amphibians, the

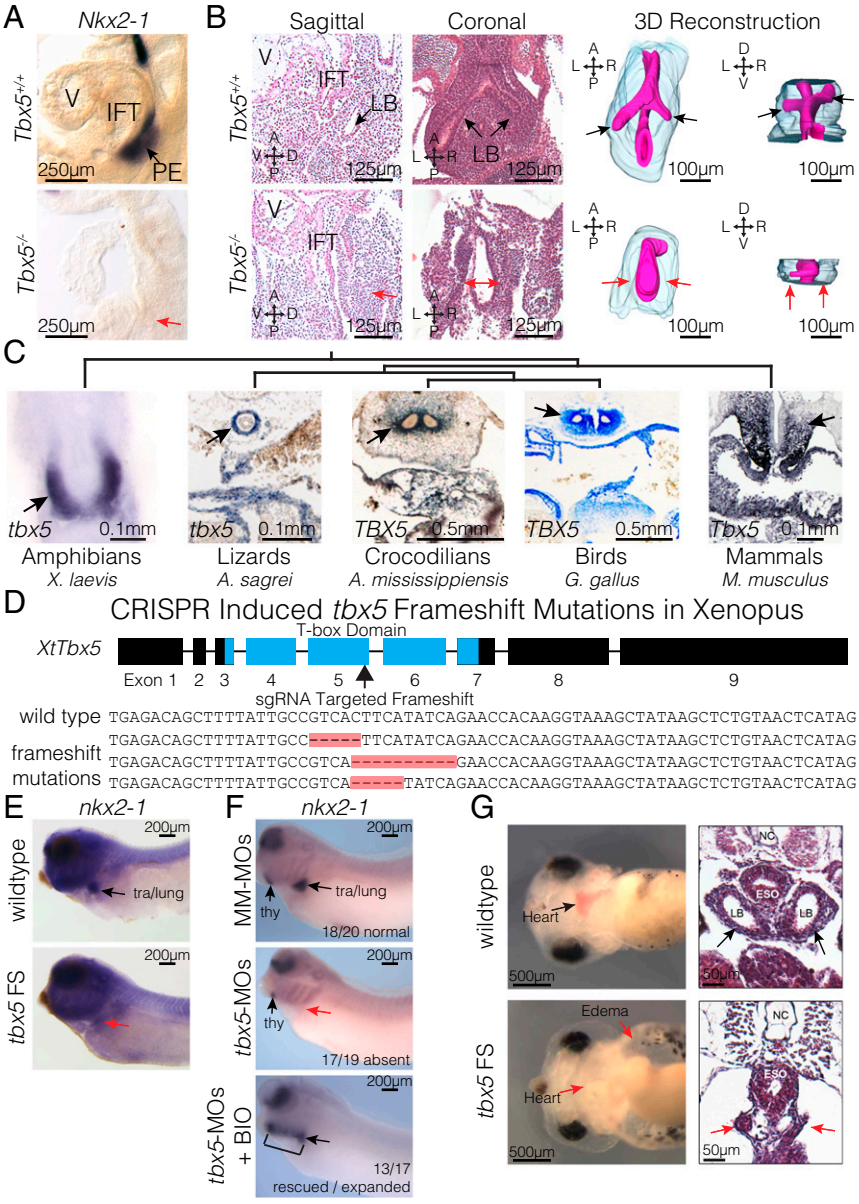

Fig. 2. *Tbx5* is required for lung development in mice and frogs. (*A*) RNA ISH for *Nkx2-1* in E9.5 $Tbx5^{+/+}$ and $Tbx5^{-/-}$ embryos. The PE, inflow tract (IFT), and cardiac ventricle (V) are labeled. (*B*) Histology from both sagittal and coronal perspectives (*Left*) and 3D reconstruction (*Right*) of E10.5 lungs from $Tbx5^{+/+}$ and $Tbx5^{-/-}$ embryos. Black and red arrows point to the lung bud (LB) branches or lack of branches off the foregut. (*C*) ISH stains of *Tbx5* across vertebrate species. Arrows indicate expression in the mesodermal derivatives surrounding the PE. (*D*, *Upper*) Strategy for generating biallelic frameshift mutations using sgRNA targeted to the fifth exon of *X. tropicalis* to disrupt the T-box domain. (*Lower*) Examples of sequences recovered from *tbx5* FS mutants. (*E* and *F*) RNA ISH of NF35 tadpoles for *nkx2-1* in wild type and *tbx5* FS mutants (*E*) and tadpoles injected with mismatched morpholinos (MM-MOs), *tbx5*-MOs, or *tbx5*-MOs cotreated with BIO (*F*). (*G*) Live images (*Left*) and H&E-stained transverse sections (*Right*) of NF42 tadpoles, depicting anatomical defects induced by CRISPR-mediated mutation of *tbx5*.

oldest lineage of extant tetrapods (32, 34). *Xenopus* embryos expressed *tbx5* in the heart and in the *wnt2b*-expressing lateral plate mesoderm surrounding the *nkx2-1*– and *shh*-expressing PE (*SI Appendix*, Fig. S1). We examined the requirement of *tbx5* for lung development in *Xenopus tropicalis* by utilizing CRISPR to induce targeted biallelic frameshift mutations in the fifth exon of *tbx5* (termed "*tbx5* FS"), causing predicted truncations of the Tbx5 polypeptide due to premature translation termination (Fig. 2*D*). We observed a loss of *nkx2-1* in the foregut endoderm of *tbx5* FS embryos compared with controls by ISH of embryos at stage 35, when the lung lineage is being induced (Fig. 2*E*). We observed an identical loss of *nkx2-1* in *X. laevis* embryos injected with *tbx5* morpholinos (MOs) (Fig. 2*F*). *tbx5* FS embryos appear phenotypically similar to previously described *tbx5*-MO knockdowns at stage 42 (35, 36), including gross edema and loss of blood in the embryonic heart (Fig. 2*G*). Furthermore, similar to the $Tbx5^{-/-}$ mouse (22), *tbx5* FS embryos lacked lung buds as determined by histologic section at stage 42 (Fig. 2 *B* and *G*). To further characterize lung development, expression of *sftpc*, encoding surfactant protein C and a marker of pulmonary epithelium, was examined (6, 37). *Sftpc* expression was absent from the lung buds of *tbx5*-MO knockdowns at stage 42 but was rescuable by coinjection with a hormone-inducible version of Tbx5 (GR-Tbx5) (*SI Appendix*, Fig. S2). Together, these data indicated that *Tbx5*-dependent PE specification is evolutionarily ancient and is conserved from amphibians to mammals.

The SB of ray-finned fish is an endoderm-derived out-pocket proposed to be a lung homolog and whose development shares many genetic pathways with lung development, including Wnt- and Hh-dependent signaling and transcriptomes (38–44). The role of *Tbx5* in heart and limb development of ray-finned fish is conserved with tetrapods (45–47). To address whether *Tbx5* is required for SB formation, zebrafish homozygous for the *tbx5a* mutant *heartstrings* (*hst*) allele (45) were examined at 96 h postfertilization (hpf). Similar to clutchmate controls, homozygous *hst* mutants show SB formation (*SI Appendix*, Fig. S3). Zebrafish have two copies of the *Tbx5* gene, *tbx5a* and *tbx5b* (48). To address potential redundancy, we utilized published MOs designed to target *tbx5a*, *tbx5b*, or *tbx5a* and *tbx5b* (47, 48). In all conditions, early expression of *shha* in the SB bud at 72 hpf (39) and SB formation at 96 hpf was observed (*SI Appendix*, Fig. S3). Together, our data suggest that, while *Tbx5* is

required for the initiation and formation of the lungs, *tbx5a/b* is not required for the formation of the SB.

Non–Cell-Autonomous Requirement of *Tbx5* for PE Specification. Previous work in mice has demonstrated that *Nkx2-1* expression in the foregut endoderm is regulated through canonical Wnt signaling, specifically *Wnt2* and *Wnt2b*. Furthermore, temporal deletion of *Tbx5* from cultured embryos demonstrated decreased *Wnt2* and *Wnt2b* expression (22), making the Wnt ligands excellent candidates for direct TBX5 regulation. *Wnt2* and *Wnt2b* are coexpressed with *Tbx5* in the SHF mesoderm and are significantly down-regulated in $Tbx5^{-/-}$ CPPs (Fig. 1 *C* and *D*) (5, 17, 20). We examined the epistatic requirement for *tbx5* and canonical Wnt signaling in *Xenopus* lung specification. We asked if lung specification in *tbx5*-MO embryos could be rescued by activating the canonical Wnt pathway, using treatment with a glycogen synthase kinase 3 (GSK-3) inhibitor, 6-bromoindirubin-30-oxime (BIO), which stabilizes β-catenin. We found that BIO treatment rescued and expanded *nkx2-1* expression in *tbx5*-MO embryos (Fig. 2*E*), suggesting that canonical Wnt signaling is downstream of *tbx5* in the lateral plate mesoderm of amphibians. Furthermore, we observed that expression of *Wnt2* and *Wnt2b* was extinguished in $Tbx5^{-/-}$ mouse embryos at E9.5 (Fig. 3*A*) and found by ISH that *wnt2b* was similarly lost from stage-35 *tbx5* FS *X. tropicalis* and from *tbx5*-MO–injected *X. laevis* (Fig. 3 *B* and *C*). These observations were consistent with a requirement for *Tbx5* upstream of canonical Wnt signaling for pulmonary specification.

***Tbx5* Is Required for Pulmonary Shh Signaling.** Hh signaling from the PE is required for both cardiac and lung morphogenesis (7, 9, 19, 49). Specifically, *Shh* is expressed in the PE and is required for atrial septation and lung morphogenesis postinduction (8, 50, 51). We predicted that the requirement of *Tbx5* for PE specification would also reflect a requirement for pulmonary Shh signaling. We observed by RNA-seq that *Shh* is dramatically down-regulated in $Tbx5^{-/-}$ embryos, and we observed by ISH that *Shh* is specifically lost from the foregut/PE at E9.5 (Figs. 1*A* and 3*A*). This suggests that the epistatic relationship between *Tbx5* and Shh signaling (9) is an indirect feature of the requirement of *Tbx5* for pulmonary lung induction.

TBX5 haploinsufficiency in humans results in the congenital HOS, displaying radial forelimb and congenital heart defects, most commonly atrial septal defects (10–12). *Shh* expression in the PE is required for morphologic development of the atrial septum (8, 16), and we have demonstrated a genetic interaction between *Tbx5* and *Shh* (7, 9). We therefore hypothesized that a quantitative decrement in *Tbx5* would result in diminished Wnt and Shh signaling, contributing to the *Tbx5*-haploinsufficient phenotype. We examined the gene-expression level of the canonical Wnts, PE specification, and Hh signaling in mouse embryos with *Tbx5* haploinsufficiency (Fig. 3*D*). In the CPPs of $Tbx5^{+/-}$ embryos, we observed a significant down-regulation of *Wnt2* (0.67 ± 0.05 SEM, $P = 0.0126$) but not of *Wnt2b* or *Nkx2*-1 (0.69 ± 0.15 SEM, $P = 0.1707$ and 0.80 ± 0.15 SEM, $P = 0.5420$, respectively). However, a significant down-regulation of *Shh* (0.46 ± 0.04 SEM, $P = 3.693E\text{-}05$) and the canonical Hh targets *Gli1* and *Hhip* (0.81 ± 0.04 SEM, $P = 0.0347$ and 0.63 ± 0.05 SEM, $P = 0.0028$, respectively) was observed in $Tbx5^{+/-}$ embryos compared with controls. Thus, *Tbx5* haploinsufficiency caused a decrement of both *Shh* expression in the PE and Shh signaling reception in CPPs.

A Mesoderm–Endoderm–Mesoderm Signaling Loop for Cardiopulmonary Development. *Tbx5* and Shh signaling coordinately control gene expression in the CPPs for cardiac development (7, 9, 49). We asked if *Tbx5* and Shh signaling interact to regulate lung development. Previously we showed that Shh reception in CPPs promotes *wnt2b* expression during lung induction in *Xenopus* (19). We observed similar results in mice: *Wnt2b*, but not *Wnt2*, in CPPs was *Shh* dependent at E9.5 (Fig. 3*E*). We further confirmed *Wnt2* expression in the embryonic mesoderm of the $Smo^{-/-}$ germline mutant, which ablates all Hh signaling independent of ligand (*SI Appendix*, Fig. S4). These data suggest that *Wnt2* expression is upstream or independent of *Shh*, while *Wnt2b* is downstream of *Shh*.

Utilizing a suite of biochemical reagents and the *Xenopus* model (Fig. 4*A*), we investigated the interaction between Tbx5 and Shh signaling for *wnt2b* expression. RNA encoding a fusion protein between Tbx5 and the hormone-inducible region of the glucocorticoid receptor (GR-Tbx5), affording dexamethasone (DEX)-dependent regulation of nuclear import, was injected into the anterior mesendoderm (AME), which has active Hh signaling and gives rise to the foregut (52–55), or into the posterior mesendoderm (PME), which does not have active Hh signaling (Fig. 4 *A* and *B*). AME and PME tissue was explanted postgastrulation, DEX treated, and examined after 6 h (Fig. 4 *C* and *D* and *SI Appendix*, Fig. S5). We found that GR-Tbx5 was sufficient to activate *wnt2b* in the Hh-positive AME

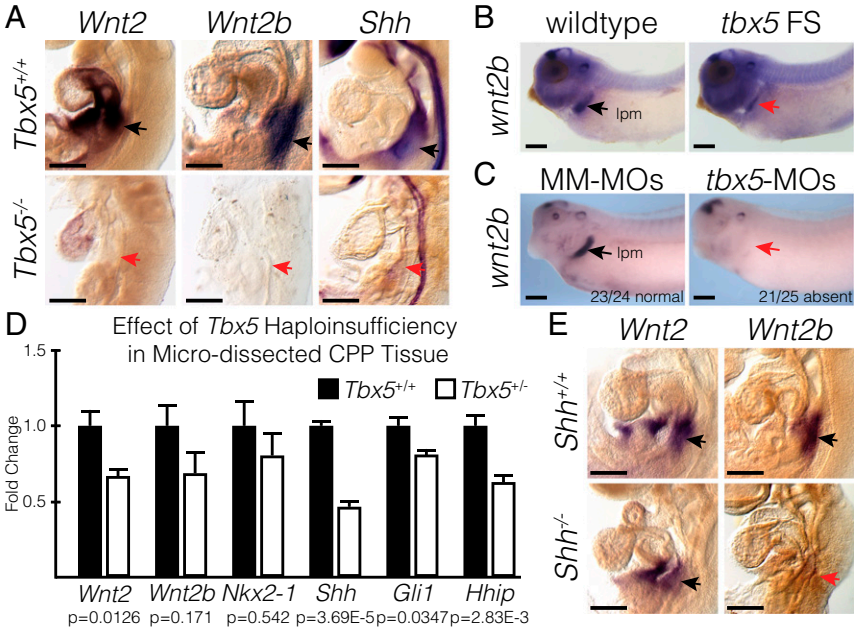

Fig. 3. *Tbx5* is required for *Wnt2/2b* and *Shh* expression. (*A*) RNA ISH for *Wnt2*, *Wnt2b*, and *Shh* in E9.5 $Tbx5^{+/+}$ and $Tbx5^{-/-}$ mouse embryos. Black and red arrows point to positive and negative staining, respectively, in the lung-forming region. (*B* and *C*) RNA ISH for *wnt2b* performed in wild-type or *tbx5* FS NF35 tadpoles (*B*) and in NF35 tadpoles injected with mismatched morpholinos (MM-MOs) or *tbx5*-MOs (*C*). The stained region corresponds with the lateral plate mesoderm (lpm). (*D*) qRT-PCR of microdissected CPP tissue from E9.5 $Tbx5^{+/+}$ or $Tbx5^{+/-}$ mouse embryos. (*E*) RNA ISH for *Wnt2* and *Wnt2b* in E9.5 $Shh^{+/+}$ and $Shh^{-/-}$ mouse embryos. (Scale bars: 250 μm.)

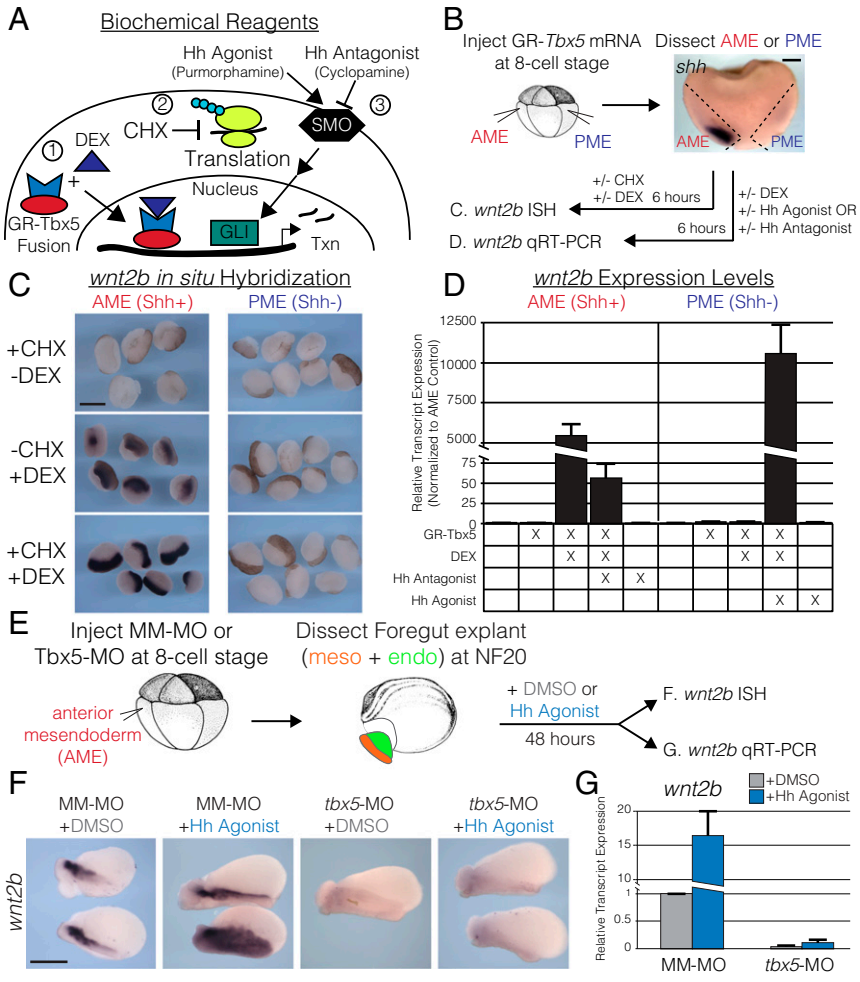

Fig. 4. *tbx5* directly regulates *wnt2b* expression for lung development in the presence of Hh signaling. (*A*) To study the interaction of Tbx5 and Hh signaling, we utilized (1) a DEX-inducible GR-Tbx5 fusion protein; (2) CHX to inhibit protein synthesis; and (3) pharmacological agonists (purmorphamine) and antagonists (cyclopamine) of Smoothened (SMO) to activate or repress Hh signaling. (*B*) Strategy used in *C* and *D* for examining the regulation of *wnt2b* by Tbx5 in the presence or absence of Shh signaling in *Xenopus*. The AME (red) corresponds to *shh*-expressing tissue, and the PME (blue) corresponds to *shh*-negative tissue. (*C*) RNA ISH for *wnt2b* in AME or PME explants treated with CHX, DEX, or both. Note that the ISH signal is black; the brown color is pigment. (*D*) qRT-PCR of *wnt2b* in AME or PME explants, with or without GR-Tbx5, and treated with combinations of DEX, Hh agonist, and Hh antagonist. (*E*) Strategy used in *F* and *G* to examine the regulation of *wnt2b* by Hh signaling in the presence or absence of *tbx5*. AME explants were treated with DMSO (gray) or the Hh agonist purmorphamine (blue) for 48 h. (*F*) RNA ISH for *wnt2b* on DMSO- or Hh agonist-treated explants from embryos injected with mismatched morpholinos (MM-MO) or *tbx5*-MO. (*G*) qRT-PCR of *wnt2b* normalized to DMSO-treated MM-MO–injected explants. (Scale bars: *B*, 200 μm; *C* and *E*, 400 μm.)

but not in the Hh-negative PME (Fig. 4 *C* and *D*). We examined whether *wnt2b* activation by GR-Tbx5 was direct by coadministering DEX with cycloheximide (CHX) to block translation (Fig. 4 *A*–*C*). As with DEX administration alone, DEX/CHX coadministration induced *wnt2b* expression in the AME but not in the PME (Fig. 4*B*), suggesting that GR-Tbx5 directly activates *wnt2b* expression in Hh-positive tissue. To validate the requirement for Hh signaling, we coadministered DEX with the Hh antagonist cyclopamine (*SI Appendix*, Fig. S5) (56). Coadministration of DEX and cyclopamine significantly blunted the activation of *wnt2b* in AME tissue as compared with DEX alone (97.0-fold decrement, $P = 5.48E\text{-}3$) (Fig. 4*D*). Last, we examined whether Hh signaling in the AME was unique or whether treatment of PME tissue with the Hh agonist purmorphamine (57) was sufficient for the coinduction of *wnt2* expression. PME tissue treated with purmorphamine alone significantly activated *gli1* (16.7-fold activation, $P = 0.015$) but not *wnt2b* (Fig. 4*D* and *SI Appendix*, Fig. S5). However, injection of GR-Tbx5 followed by coadministration of DEX and purmorphamine significantly activated *wnt2b* expression in the PME ($P = 9.29E\text{-}3$) (Fig. 4*D*). Together, these data suggested that Tbx5 directly activates *wnt2b* gene expression in the presence of active Hh signaling.

We next evaluated whether Tbx5 is required for the Hh pathway to activate expression of *wnt2b* and other markers of pulmonary development (Fig. 4 *E*–*G* and *SI Appendix*, Fig. S5). We activated Hh signaling using the Hh agonist purmorphamine in control or *tbx5*-MO–injected AME foregut explants (Fig. 4*E*). Purmorphamine treatment of control embryos expanded the endogenous *wnt2b* expression domain, consistent with activation by Hh signaling (Fig. 4 *F* and *G*). However, purmorphamine was unable to promote *wnt2b* in explants from *tbx5*-MO embryos, which, similar to vehicle-treated *tbx5*-MO explants (Fig. 4 *F* and *G*), had little detectable *wnt2b*. Similar to $Tbx5^{-/-}$ mice (Figs. 1 and 3), *tbx5*-MO explants displayed decreased expression of *nkx2-1* ($P = 1.13E\text{-}9$), *shh* ($P = 6.81E\text{-}3$), and *dhh* ($P = 1.11E\text{-}5$) in the foregut endoderm and decreased expression of *wnt2b* ($P = 1.20E\text{-}3$) and *gli1* ($P = 1.09E\text{-}3$) in the mesoderm (Fig. 4 *F* and *G* and *SI Appendix*, Fig. S5). These explant data demonstrate that *tbx5* and Hh signaling are corequired for *wnt2b* expression and further demonstrate that *Tbx5* expression is required for *Shh* and *dhh* expression in the PE. Overall, these findings suggest a hierarchical series of signaling loops: TBX5 drives canonical Wnt mesoderm-to-endoderm signaling for pulmonary induction, and Shh signaling from the PE to mesoderm collaborates with mesodermal TBX5 to drive ongoing WNT2B mesoderm-to-endoderm signaling for pulmonary morphogenesis.

Identification of TBX5-Dependent *Wnt2* Enhancers. To identify direct targets of TBX5 in coordinating cardiopulmonary specification, we performed TBX5 ChIP-seq on microdissected hearts including the *Wnt2*-expressing inflow tract from E9.5 mouse embryos (Fig. 1*A*). We identified 3,883 TBX5-bound regions at E9.5 (Fig. 5*A* and *SI Appendix*, Table S2). These locations segregated into 823 promoter-proximal (TBX5 summit ≤2 kbp from an annotated transcription start site) and 3,060 promoter-distal sites. To define TBX5 binding in a genomic context, we identified active promoters and *cis*-regulatory regions for H3K4me3 and H3K4me1 by ChIP-seq and in microdissected E9.5 heart and CPP tissue by assay for transposase-accessible chromatin sequencing (ATAC-seq) (Figs. 1*A* and 5*A*) (58). ATAC-seq, genome-wide and at TBX5-bound regions, showed similar signal (Pearson

DEVELOPMENTAL BIOLOGY

correlation coefficient = 0.96 and 0.93), H3K4me1 (Pearson correlation coefficient = 0.89 and 0.76), and H3K4me3 (Pearson correlation coefficient = 0.92 and 0.93) in both CPPs and the heart (*SI Appendix*, Fig. S6). To identify direct TBX5 targets in the CPP tissue, we overlapped the 1,480 *Tbx5*-dependent genes (Fig. 1*C*) with the 3,880 ChIP sites (annotated to the nearest gene). This conservative approach identified 162 genes associated with 220 bound sites, including *Wnt2* and *Wnt2b* (Fig. 5 *B* and *C* and *SI Appendix*, Fig. S7 and Table S3). This observation was consistent with the hypothesis that TBX5 directly regulates *Wnt2* and *Wnt2b* transcription (22, 32).

While both *Wnt2* and *Wnt2b* are *Tbx5* dependent and redundant for lung development (17, 22), only *Wnt2* is required for both lung and cardiac morphogenesis in mammals (18). Therefore, we attempted to identify the TBX5-dependent *cis*-regulatory elements that control *Wnt2* expression. We compared our TBX5 ChIP-seq results with previously published TBX5 ChIP-seq from two in vitro systems (59, 60). Using this approach, we identified a cluster of TBX5-bound sites adjacent to the 3′ end of the neighboring gene, *St7*, which demonstrated the hallmarks of putative regulatory elements including chromatin accessibility and H3K4me1 signal (Fig. 5*C*). We cloned the regions corresponding to the ChIP-seq signal (mm10 chr6:17938154–17940081, chr6:17941997–17942724, and chr6:17952290–17953703) and named the putative regulatory elements "*Wnt2* enhancer 1," "*Wnt2* enhancer 2," and "*Wnt2* enhancer 3" (W2E1–3), respectively (Fig. 5*C*). We performed ChIP-qPCR in IMR90 human lung fibroblast cells to validate TBX5 localization at these candidate enhancers (Fig. 5*D*). We observed a significant enrichment of TBX5 at W2E1 and W2E2 over IgG control (12.14 ± 3.81 SD, $P = 0.03$ and 10.95 ± 0.85 SD, $P = 3.5E\text{-}5$, respectively), while W2E3 did not show enrichment (0.58 ± 0.36 SD, $P = 0.44$).

We examined the enhancer activity and *Tbx5* dependence of W2E1–3 in vitro by luciferase reporter assay using HEK293T cells and exogenous expression of *Tbx5*, as previously described (7, 8, 61). *Tbx5* expression activated W2E1 and W2E3 (3.44 ± 1.07 SEM, $P = 0.0309$ and 5.29 ± 0.93 SEM, $P = 0.0099$, respectively) but not W2E2 (1.27 ± 0.33 SEM, $P = 0.4532$) compared with a control vector (Fig. 5*E*). As W2E1 was both TBX5 bound and responsive to *Tbx5* expression, we examined the dependence of W2E1 activity on the presence of the canonical T-box motif AGGTG (*SI Appendix*, Fig. S8) (59, 60, 62). Mutation of the minimal canonical T-box motifs in W2E1 resulted in a 3.997-fold decrease compared with wild-type W2E1 ($P = 0.0252$), whereas mutation of T-box motifs within the control vector had no effect ($P = 0.5237$).

We examined the sufficiency of W2E1–3 for driving cardiac and SHF gene expression in vivo. Each enhancer was cloned upstream of the *Hsp68* minimal promoter driving *lacZ* expression and was utilized for the generation of transient transgenic

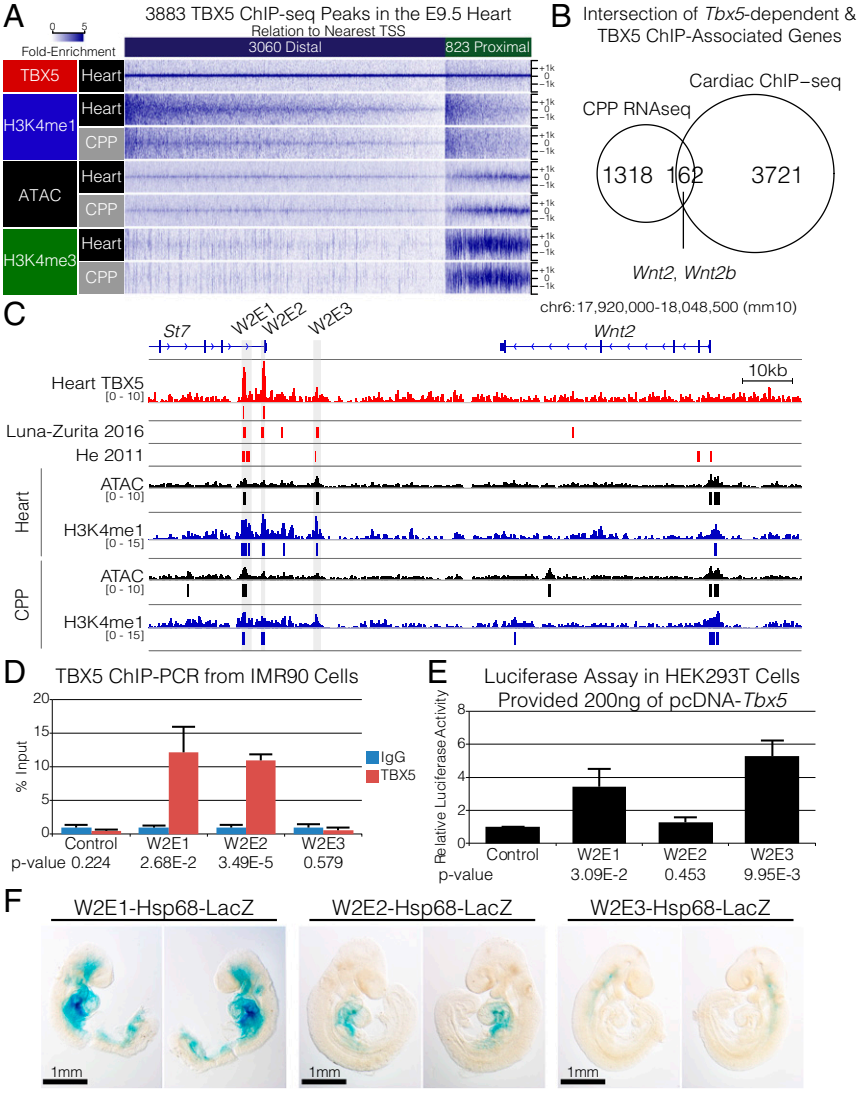

Fig. 5. Identification of TBX5-bound *cis*-regulatory elements for *Wnt2*. (*A*, *Upper*) We identified 3,883 peaks by TBX5 ChIP-seq in the E9.5 heart that correspond to 3,060 distal and 823 proximal sites. (*Lower*) Heatmaps of fold enrichment plotted for TBX5, H3K4me1, and H3K4me3 by ChIP-seq and ATAC-seq from the heart and CPP microdissections at each of the 3,883 summits ± 2,000 bp. (*B*) Overlap of the 1,318 down-regulated genes in the CPP of *Tbx5*$^{-/-}$ embryos by RNA-seq and the 3,883 genes nearest to TBX5 ChIP-seq peaks. The 162 genes in the intersection include *Wnt2* and *Wnt2b*. (*C*) Genome browser view of *Wnt2* and *St7* (mm10 chr6:17,920,000–18,048,500) with TBX5 ChIP-seq (both from *A* and published in refs. 59 and 60), H3K4me1 ChIP-seq, and ATAC-seq in the heart and pSHF. Tracks depict fold-enriched signal, and bars below represent significant peak calls. Cloned enhancers W2E1, -2, and -3 are shaded in gray. (*D*) ChIP-PCR for TBX5 at W2E1, -2, and -3 in the human IMR90 lung fibroblast cell line. Significance is calculated relative to IgG control. (*E*) Luciferase assay examining activation of W2E1, -2, and -3 in HEK293T cells provided a vector containing *Tbx5* relative to a control vector. (*F*) Transgenic embryos were generated using an Hsp68-LacZ reporter construct upstream of W2E1, -2, or -3 and were stained at E9.5.

mouse embryos, as previously described (7, 63, 64). W2E1 and W2E2 each drove robust activation of *lacZ* within the CPP and inflow tract domains of *Wnt2* expression with W2E1 driving robust activation of *lacZ* within many domains of *Wnt2* at E9.5 (Fig. 5*F*). W2E3, in contrast, activated *lacZ* in non–*Wnt2*-, non–*Tbx5*-expressing tissues. Taken together, our data suggested that W2E1 and W2E2 represent TBX5-responsive *cis*-regulatory elements for early cardiopulmonary *Wnt2* expression.

Requirement of TBX5-Dependent Regulation of *Wnt2*. To investigate the direct requirement of TBX5-driven enhancers for pulmonary mesoderm gene expression, we generated a mouse embryonic stem cell (mESC) line with doxycycline (DOX)-inducible *Tbx5* expression using the A2Lox.cre mESC line (65). This line (*Tbx5*OE-mESC) was differentiated along a sequence of ES cells to mesoderm to lateral plate mesoderm to cardiac progenitor as previously described (66). We observed a linear dose-response of *Tbx5* in cardiac progenitors (0 ng/μL to 500 ng/μL; $0.07x + 0.60$, $P = 3.29E\text{-}4$) after 24 h (Fig. 6*A*). We observed a significant relationship between DOX dose and expression of *Wnt2* ($P = 1.02E\text{-}2$), *Wnt2b* ($P = 1.55E\text{-}3$), and *Tbx4* ($P = 2.03E\text{-}2$), another marker of pulmonary mesoderm. This observation suggested that pulmonary mesodermal markers are directly responsive to *Tbx5* expression levels in CPPs in vitro.

We examined the requirement of the TBX5-bound *cis*-regulatory elements W2E1 and W2E2 for *Tbx5*-dependent *Wnt2* expression. Specifically, we utilized CRISPR/cas9 to generate a 4.6-kbp deletion of W2E1 and W2E2 without disrupting the last exon of *St7* or its predicted splice acceptor from the mESC line overexpressing *Tbx5* (hereafter, the "*Tbx5*OE-mESC line") (Fig. 6*B*). Two homozygous deletion clones (W2E mutants) and two control clones (W2E controls) were generated and evaluated. Following differentiation of clones to cardiac progenitors, the W2E mutants demonstrated a significant reduction in *Wnt2* gene expression compared with W2E controls (91.8% reduction, $P = 0.0122$), while there was no significant difference in *Tbx5* or *St7* (Fig. 6*C*). To examine the requirement of W2E1/W2E2 for *Tbx5*-dependent activation of *Wnt2*, we induced *Tbx5* overexpression and evaluated the response of *Tbx5*, *Wnt2*, and *St7* expression. We observed that the W2E mutants had significantly reduced *Wnt2* expression in response to *Tbx5* overexpression compared with the W2E control lines (2.31-fold versus 1.28-fold activation, $P = 0.0150$); no significant differences between the mutant and control lines were observed for *Tbx5* or *St7* (Fig. 6*D*). Taken together, these results demonstrate that W2E1 and W2E2 are required for *Wnt2* expression and are necessary for *Tbx5*-responsive *Wnt2* expression in mESC-derived CPPs. These results demonstrate direct molecular control of *Wnt2* by TBX5 in an in vitro model of early cardiopulmonary development.

Discussion

TBX5 has been genetically implicated in human cardiac septal defects for over 20 y. Based on its strong expression in the heart, *TBX5* was assumed to directly drive a cardiac GRN for cardiac septation. Recently, work by the I.P.M. laboratory has determined that the role of *TBX5* resides in the SHF (Fig. 7). We assumed that probing pSHF CPPs for *Tbx5*-dependent target genes would uncover a direct cardiac progenitor GRN for cardiac morphogenesis. Instead, we observed a primary role for *Tbx5* in the initiation of lung development and, secondarily, the establishment of PE-to-mesoderm signaling for cardiac septation.

We report that *Tbx5* is required for the initiation of lung development through canonical Wnt signaling (Fig. 7). We observed that *Tbx5* directly regulates the transcription of both *Wnt2* and *Wnt2b*, wingless-family signaling molecules redundantly required for the earliest aspects of pulmonary development (17). Specifically, we identified *cis*-regulatory elements for *Wnt2* that are required for TBX5-responsive transcription and that drive transcription in the CPPs and inflow tract of the heart. A role for canonical Wnt signaling in inflow tract development is conserved between *Drosophila* and mammals (67). *Drosophila Wingless* (*wg*)

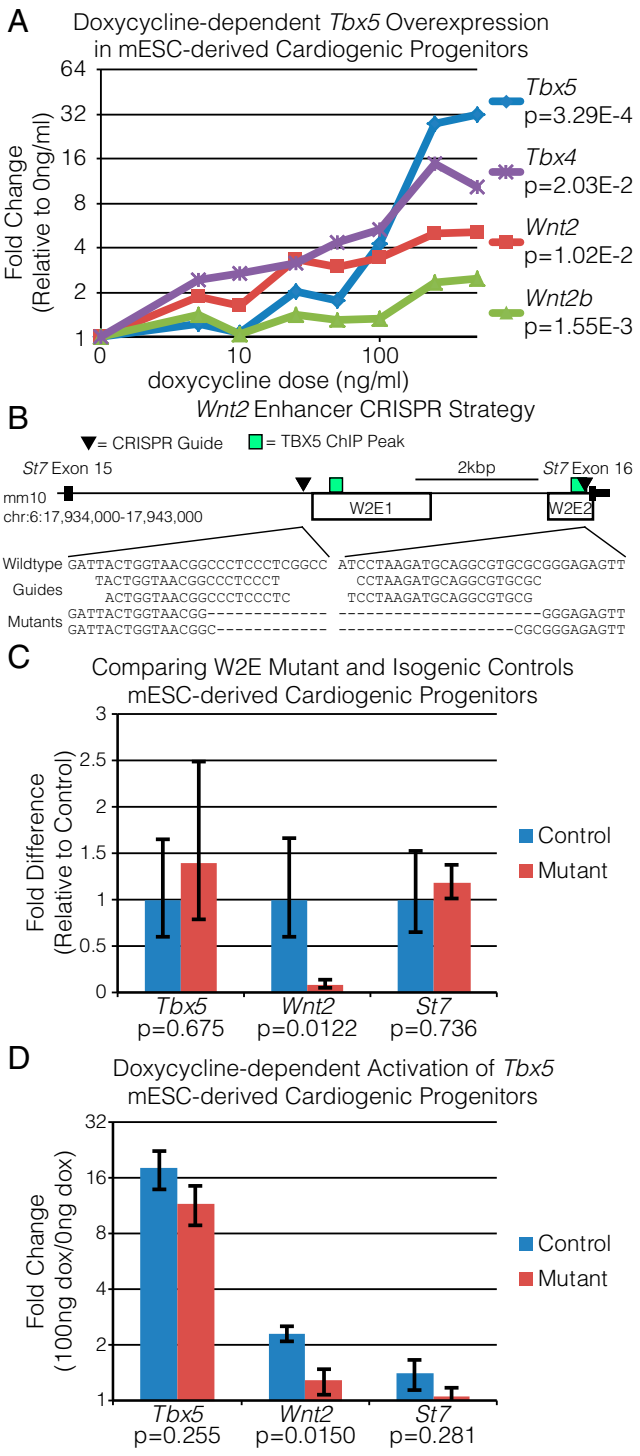

Fig. 6. *Cis*-regulatory elements are required for *Wnt2* expression. (*A*) Dose-dependent gene-expression changes in mESC-derived cardiogenic progenitors harboring a DOX-dependent *Tbx5* construct (*Tbx5*OE-mESC) measured by qRT-PCR. Cells were treated with DOX for 24 h before analysis. (*B*, *Upper*) sgRNAs were designed to induce a 4.5-kb deletion within the last intron of *St7*, removing a majority of W2E1 and W2E2 in the *Tbx5*OE-mESC via CRISPR-Cas9. This design maintains the last exon and the predicted splice branch for *St7* while removing the TBX5-bound sites in W2E1 and W2E2. (*Lower*) Amplification and sequencing across the target site demonstrate successful deletion. (*C*) Expression levels of *Tbx5*, *Wnt2*, and *St7* were compared in W2E mutants and isogenic controls following differentiation to cardiogenic progenitors by qRT-PCR. (*D*) Changes in *Tbx5*, *Wnt2*, and *St7* expression following 24 h of 100 ng/mL DOX relative 0 ng/mL DOX in the W2E mutant and isogenic controls differentiated to cardiogenic precursors.

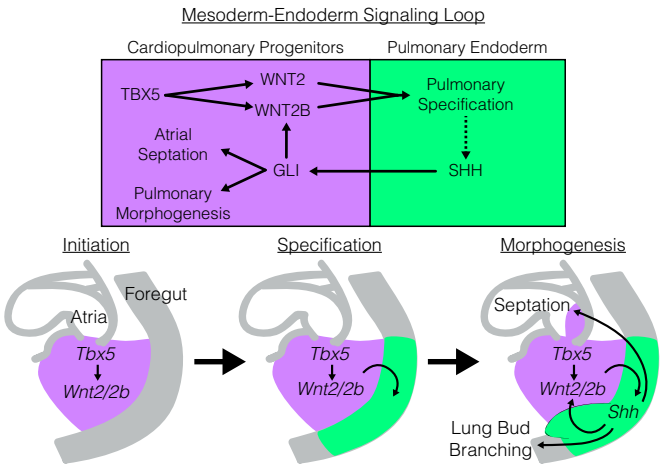

Fig. 7. *Tbx5* is required for a mesoderm–endoderm bidirectional signaling loop for cardiopulmonary development. Model of genetic interaction between *Tbx5*, canonical Wnt signaling, and Hh signaling for PE specification, pulmonary morphogenesis, and cardiac septation. TBX5, expressed in the CPPs (purple) initiates the bidirectional signaling loop through direct activation of *Wnt2* and *Wnt2b* expression. Canonical Wnt signaling drives pulmonary specification in the foregut endoderm and *Nkx2-1* expression. SHH, derived from the PE (green) signals back to the CPPs where it cooperatively activates *Wnt2b* but not *Wnt2*. Shh signaling drives both atrial septation and lung bud morphogenesis through previously described downstream targets.

is required for the formation of the *Drosophila* cardiac inflow tract (67), suggesting that the preexisting role of canonical Wnt signaling in inflow tract development may have been coopted for lung development and inflow septation later in vertebrates and early tetrapods. Although the early requirement of *Tbx5* for heart and limb development has been well documented across vertebrate species (13–15, 45–47, 68–70), the role of *Tbx5* in lung development has not been examined outside of mammals. Overall, our work suggests a fundamental role for *Tbx5* in tetrapod lung development and the possibility that the evolutionary origin of lungs may have involved the recruitment of TBX5 from an ancestral cardiac expression domain.

Although a recent model suggested that the lungs and SB are evolutionarily derived from a common structure, we find that *tbx5* is not required for the development of both (43, 44). Previous work in zebrafish demonstrates that depletion of *wnt2* and *wnt2bb* causes SB agenesis, similar to their requirement in lung specification (17, 38). However, we find that although *Tbx5* is required for lung formation, *tbx5a/b* is not required for SB formation in the zebrafish. These observations suggest that *tbx5a/b*-independent regulation of Wnt signaling is required for the initiation of SB development. One question worth future investigation is whether the Tbx5-positive lateral plate mesoderm gives rise to SB components or whether the dorsally derived SB forms from a mesodermal contribution distinct from the ventrally derived lungs. Additionally, zebrafish are part of the derived teleost fish, and further characterization across ray-finned fish is required. We note that the Senegal bichir (*Polypterus senegalus*), a member of the early-diverging Actinopterygii, has a ventral-sided lung structure for air breathing and was reported to express both *tbx5* and *tbx4* in the early lung structure (43). Additional work is required to resolve the evolutionary relationship between the SB and lungs.

Integrating our observations that *Tbx5* is required for pulmonary specification with previous work demonstrating a role for *Tbx5* in lung morphogenesis (22) suggests sequential roles for Wnt signaling during lung development: an early requirement for initiation and a later requirement for branching morphogenesis. In contrast to the complete loss of lung development in the *Tbx5* germline-null mouse, conditional removal of *Tbx5* at E8.5 caused malformation of lung bud branching and disruption of canonical Wnt signaling in explant cultures (22). Consistent with a dual-role hypothesis, a partial decrement of canonical Wnt signaling allows lung initiation but causes defects in lung-branching morphogenesis (17, 18), while a complete failure of lung initiation has been observed only by homozygous removal of both *Wnt2* and *Wnt2b* (17). We conclude that *Tbx5* initiates a multistep mesoderm–endoderm–mesoderm signaling loop (Fig. 7). TBX5 directly drives WNT2 and WNT2B mesoderm-to-endoderm signaling for pulmonary induction. Secondarily, PE-to-mesoderm Shh signaling collaborates with mesodermal TBX5 for ongoing WNT2B mesoderm-to-endoderm signaling and later pulmonary morphogenesis (Fig. 7).

This study and previously published work suggest that *TBX5* mutations may be associated with lung defects. Although rare, lung defects have been described in patients with HOS. Two cases of structural lung disease have been associated with "atypical" HOS: one case of right lung agenesis (71) and one case of horseshoe lungs (72). Additionally, a screen of patients with esophageal atresia and tracheoesophageal fistula identified a patient with HOS (73). Further, rare genetic variants at the *TBX5/RBM19* locus have been associated with lung function in smokers by a genome-wide association study (74). These studies suggest the intriguing possibility that *TBX5* may play a role in both lung development and adult lung function, similar to its requirement for both cardiac development and adult cardiac function (15, 61, 63, 75).

Cardiac septa are observed in all lunged vertebrates. We have previously demonstrated that GLI-dependent transcription downstream of PE Shh signaling and *Tbx5* cooperate in mesodermal SHF CPPs to drive atrial septation (7–9, 49). Here, we demonstrate that *Tbx5* is required for the initiation of Shh signaling through the specification of PE. Previous work demonstrated that atrial septal defects caused by removal of *Tbx5* from the CPPs were rescued by concomitant activation of Hh signaling in those cells, providing epistatic evidence that *Tbx5* acts upstream of Hh signaling for atrial septation (9). In this context, our current results suggest that Shh signaling from the PE to the CPPs is a direct requirement for atrial septation, while *Tbx5* may be dispensable following the initiation of lung development and subsequent Shh signaling. Our work demonstrates that *Tbx5* haploinsufficiency causes reduced *Wnt2* expression and subsequently reduced expression of *Shh* in the PE, resulting in reduced expression of quantitative markers of Shh reception in the cardiopulmonary mesoderm. Therefore, this quantitative decrement in CPP Hh signaling may contribute to the causation of cardiac septal defects in HOS patients.

The linked mesoderm–endoderm–mesoderm molecular pathways for lung development and cardiac inflow septation are conserved between amphibians and mammals. Remarkably, amphibians with evolutionary loss of lungs exhibit much reduced atrial septation, consistent with necessary instructive cross-talk between these structures (3, 76). We posit that *Tbx5–Wnt2/Wnt2b* signaling provides a molecular basis for the link between lung formation and the cardiac specializations required for pulmonary blood flow observed in lunged vertebrates.

Materials and Methods

Ethics Statement. All murine and zebrafish experiments were performed under University of Chicago Institutional Animal Care and Use Committee (IACUC) protocols no. 71737 and no. 71112. *X. laevis* and *X. tropicalis* adults were housed according to Cincinnati Children's Hospital Medical Center or University of North Carolina, Chapel Hill IACUC protocols. Handling of lizards (*Anolis sagrei*) and harvest of tissues complied with national and institutional guidelines and were approved by the IACUC of the University of Amsterdam (DAE101617).

Mouse Lines. *Tbx5* germline mutant animals ($Tbx5^{+/-}$) were produced by crossing the $Tbx5^{tm1Jse}$ allele ($Tbx5^{flox}$) with a germline cre-recombinase and were out-crossed for multiple generations with CD1 animals as previously described (15, 23). Additionally, the Shh^{tm1Amc} (77) and Smo^{tm1Amc} (78) germline mutants have been previously described.

***Xenopus* Experiments and CRISPR-Based Genome Editing.** Ovulation, in vitro fertilization, and dejellying of embryos were performed as described (79). The pCS2+GR Tbx5 plasmid (70) was used to synthesize mRNA for injection using the Ambion mMessage mMachine SP6 RNA synthesis kit. GR-Tbx5 RNA (125 pg) was injected into either the dorsal or ventral marginal zone (targeting the AME or PME, respectively) at the eight-cell stage. Validated Tbx5 translation-blocking MOs (35) were injected at the eight-cell stage (3.5 ng of each MO). See *SI Appendix* for full details.

A small guide RNA (sgRNA) designed to target exon 5 of the *X. tropicalis* locus (GGGGTTCTGATATGAAGTGA) was coinjected at 200 pg with 2 ng Cas9 protein (PNA Bio) in 2-nL drops into one-cell-stage wild-type *X. tropicalis* embryos (80). To screen rapidly for altered loci, an ∼500-bp genomic fragment asymmetrically flanking the sgRNA target sequence was amplified by PCR and subjected to digestion by T7 endonuclease (New England Biolabs).

Zebrafish Lines and Experiments. Zebrafish were maintained under standard laboratory conditions (81). MO injections were performed as described (82). *tbx5a* MO (3.7 ng) (47) and 5 ng of *tbx5b* translation-blocking MO (48) were injected into each embryo. Lines used were *AB and *heartstrings* (*hst*) mutants (45).

Transcriptional Profiling by RNA-Seq. RNA-seq was performed on microdissected CPP tissue at E9.5. Microdissected tissues from four embryos were pooled, and total RNA was extracted from five $Tbx5^{+/+}$ and two $Tbx5^{-/-}$ pools and was sequenced using the Illumina HiSeq 2500 platform by the Genomics Core Facility at the University of Chicago. Analysis was performed as previously described (23). See *SI Appendix* for full details.

qRT-PCR. For mice, RNA was extracted from microdissected tissue as was done for RNA-seq. The reverse-transcription reaction was performed using SuperScript III First-Strand Synthesis SuperMix (Invitrogen). qRT-PCR was performed using Power SYBR Green PCR master mix (Applied Biosystems) and was run on an AB7500 machine (Applied Biosystems). Gene-expression level was normalized by *Gapdh*. For *Xenopus*, RNA was collected from three biological replicates containing four explants each. RNA was extracted using the Direct-zol RNA MiniPrep Plus kit (R2070; Zymo Research), and cDNA was generated using SuperScript VILO Master Mix (11755050; Thermo Fisher). Real-time PCR reactions were carried out using PowerUp SYBR Green Master Mix (A25742; Thermo Fisher) on ABI StepOnePlus qPCR machines (Applied Biosystems). *Ornithine decarboxylase* (*odc*) was used as a reference gene.

ISH. Mouse embryonic ISH was performed as previously described (7, 83, 84). ISH of *Xenopus* embryos and explants was performed as described (79). ISH was performed on stage-11 lizards as previously described (85). The alligator and chicken sections come from a stained series used in previous publications (86, 87), but the sections shown have not been published before. See *SI Appendix* for full details.

Histology and 3D Reconstruction. All mouse and zebrafish embryonic histology was performed by the University of Chicago Human Tissue Resource Center. All tissues were fixed in formalin, embedded in paraffin wax, and sectioned to 10-μM thickness. Tissue was counterstained with H&E. Reconstructions of embryonic lung histology were performed using AMIRA (5.3.2). See *SI Appendix* for full details.

ChIP and Analysis. Chromatin extract was prepared from microdissected tissue from E9.5 CD-1 mouse embryos (2× from 50 embryo pools each) obtained from Charles River or from pelleted IMR90 cells (4× from 5 million cells each). For immunoprecipitation, the chromatin extract was incubated with anti-TBX5 antibody (sc-17866; lot no. G1516; Santa Cruz Biotechnology), anti-H3K4me3 (no. 305-34819; lot no. 14004; Wako Chemicals), or anti-H3K4me1 (ab8895; lot no. GR257926-1; Abcam). High-throughput sequencing libraries from ChIP and input DNA were prepared using the NEBNext Ultra DNA Library Prep Kit (E7370S; New England Biolabs) and were sequenced using Illumina HiSeq instruments by the Genomics Core Facility at the University of Chicago. ChIP-seq analysis was performed using a typical pipeline involving Bowtie2 (88) and MACS2 (89, 90). See *SI Appendix* for full details.

ATAC-Seq and Analysis. ATAC-seq was performed as previously described (58) on an Illumina HiSeq system by the Genomics Core Facility at the University of Chicago. Analysis was performed in a similar manner to ChIP-seq. See *SI Appendix* for full details.

Luciferase Assays. pCDNA3.1 expression vectors for *Tbx5* were previously described (63). W2E1–3 were cloned into the pGL4.23 vector (Promega). Expression and reporter vectors were transfected into HEK293T cells using FuGENE (Promega). Cells were cultured for 48 h after transfection and then were lysed and assayed using the Dual-Luciferase Reporter Assay System (Promega).

Transient Transgenics. Transient transgenic experiments were performed at E9.5 as previously described (7, 63, 64). W2E1–3 were subcloned into the Hsp68-LacZ vector. The resulting construct was digested with NotI enzyme to remove the backbone, gel-purified, and injected into fertilized mouse eggs at the University of Chicago Transgenics Core Facility.

Tbx5OE-mESC Generation, CRISPR, and in Vitro Differentiation. The inducible *Tbx5*OE-mESC line was generated as previously published (65). To generate the W2E mutants, we transfected the mESC with pSpCas9(BB)-2-Puro (PX459) plasmid vectors containing guides designed to generate an ∼4.6-kbp deletion of W2E1 and W2E2. Following clone selection and expansion, two homozygous deletion clones (W2E mutants) and two wild-type clones (W2E controls) were evaluated. Cardiac stem cell differentiation was based on the original protocol from the laboratory of Keller and coworkers (66) with some modifications. For all mESC experiments utilizing overexpression, cells were treated with DOX (Sigma D9891) at the cardiac progenitor-like stage (day 6) and were harvested for RNA 24 h later. For CRISPR cell line evaluation, a dose of 100 ng/mL was used. See *SI Appendix* for full details.

ACKNOWLEDGMENTS. We thank Lorenzo Pesce for use of the Beagle2 super computer partly supported by NIH Grant 1S10OD018495-01. This work was funded by NIH Grants R01 HL092153 and R01 HL124836 (to I.P.M.), R01 HD089275 (to F.L.C.), R01 HL126509 (to F.L.C. and I.P.M.), R01 DK070858, R01 HL114898, and P01 HD093363 (to A.M.Z.), R01 HD072598 (to R.K.H.), R01 HD084409 and P40 OD010997 (to M.E.H.), U01 HL100407 (to M.K.), R21 AG054770 (to K.I.), and R21 LM012619 (to X.H.Y.); support was also provided by NIH Grants T32 GM007183 (J.D.S.), T32 HL007381 (J.D.S., A.B.R., R.D.N., M.R., and A.D.H.), T32 HD055164 (S.L.), and T32 GM007197 (A.D.H. and E.A.T.B.A.) and by Regenerative Medicine Minnesota Grant RMM 102516 001 (to S.S.-K.C.).

1. Hsia CC, Schmitz A, Lambertz M, Perry SF, Maina JN (2013) Evolution of air breathing: Oxygen homeostasis and the transitions from water to land and sky. *Compr Physiol* 3: 849–915.
2. Farmer CG (1999) Evolution of the vertebrate cardio-pulmonary system. *Annu Rev Physiol* 61:573–592.
3. Jensen B, Spicer DE, Sheppard MN, Anderson RH (2017) Development of the atrial septum in relation to postnatal anatomy and interatrial communications. *Heart* 103:456–462.
4. Jensen B, Wang T, Christoffels VM, Moorman AF (2013) Evolution and development of the building plan of the vertebrate heart. *Biochim Biophys Acta* 1833:783–794.
5. Peng T, et al. (2013) Coordination of heart and lung co-development by a multipotent cardiopulmonary progenitor. *Nature* 500:589–592.
6. Herriges M, Morrisey EE (2014) Lung development: Orchestrating the generation and regeneration of a complex organ. *Development* 141:502–513.
7. Hoffmann AD, et al. (2014) Foxf genes integrate tbx5 and hedgehog pathways in the second heart field for cardiac septation. *PLoS Genet* 10:e1004604.
8. Hoffmann AD, Peterson MA, Friedland-Little JM, Anderson SA, Moskowitz IP (2009) Sonic hedgehog is required in pulmonary endoderm for atrial septation. *Development* 136:1761–1770.
9. Xie L, et al. (2012) Tbx5-hedgehog molecular networks are essential in the second heart field for atrial septation. *Dev Cell* 23:280–291.
10. Basson CT, et al. (1994) The clinical and genetic spectrum of the Holt-Oram syndrome (heart-hand syndrome). *N Engl J Med* 330:885–891.
11. Newbury-Ecob RA, Leanage R, Raeburn JA, Young ID (1996) Holt-Oram syndrome: A clinical genetic study. *J Med Genet* 33:300–307.
12. Holt M, Oram S (1960) Familial heart disease with skeletal malformations. *Br Heart J* 22:236–242.
13. Li QY, et al. (1997) Holt-Oram syndrome is caused by mutations in TBX5, a member of the Brachyury (T) gene family. *Nat Genet* 15:21–29.
14. Basson CT, et al. (1997) Mutations in human TBX5 [corrected] cause limb and cardiac malformation in Holt-Oram syndrome. *Nat Genet* 15:30–35.
15. Bruneau BG, et al. (2001) A murine model of Holt-Oram syndrome defines roles of the T-box transcription factor Tbx5 in cardiogenesis and disease. *Cell* 106:709–721.
16. Goddeeris MM, Schwartz R, Klingensmith J, Meyers EN (2007) Independent requirements for hedgehog signaling by both the anterior heart field and neural crest cells for outflow tract development. *Development* 134:1593–1604.
17. Goss AM, et al. (2009) Wnt2/2b and beta-catenin signaling are necessary and sufficient to specify lung progenitors in the foregut. *Dev Cell* 17:290–298.
18. Zhang Y, et al. (2008) A Gata6-Wnt pathway required for epithelial stem cell development and airway regeneration. *Nat Genet* 40:862–870.
19. Rankin SA, et al. (2016) A retinoic acid-hedgehog cascade coordinates mesoderm-inducing signals and endoderm competence during lung specification. *Cell Rep* 16:66–78.
20. Harris-Johnson KS, Domyan ET, Vezina CM, Sun X (2009) Beta-catenin promotes respiratory progenitor identity in mouse foregut. *Proc Natl Acad Sci USA* 106: 16287–16292.

21. Domyan ET, et al. (2011) Signaling through BMP receptors promotes respiratory identity in the foregut via repression of Sox2. *Development* 138:971–981.
22. Arora R, Metzger RJ, Papaioannou VE (2012) Multiple roles and interactions of Tbx4 and Tbx5 in development of the respiratory system. *PLoS Genet* 8:e1002866.
23. Waldron L, et al. (2016) The cardiac TBX5 interactome reveals a chromatin remodeling network essential for cardiac septation. *Dev Cell* 36:262–275.
24. Burnicka-Turek O, et al. (2016) Cilia gene mutations cause atrioventricular septal defects by multiple mechanisms. *Hum Mol Genet* 25:3011–3028.
25. Minoo P, et al. (1995) TTF-1 regulates lung epithelial morphogenesis. *Dev Biol* 172: 694–698.
26. Minoo P, Li C, Liu HB, Hamdan H, deLemos R (1997) TTF-1 is an epithelial morphoregulatory transcriptional factor. *Chest* 111(Suppl):135S–137S.
27. Herriges MJ, et al. (2014) Long noncoding RNAs are spatially correlated with transcription factors and regulate lung development. *Genes Dev* 28:1363–1379.
28. Lazzaro D, Price M, de Felice M, Di Lauro R (1991) The transcription factor TTF-1 is expressed at the onset of thyroid and lung morphogenesis and in restricted regions of the foetal brain. *Development* 113:1093–1104.
29. Cardoso WV, Lü J (2006) Regulation of early lung morphogenesis: Questions, facts and controversies. *Development* 133:1611–1624.
30. Warburton D, et al. (2010) Lung organogenesis. *Curr Top Dev Biol* 90:73–158.
31. McCulley D, Wienhold M, Sun X (2015) The pulmonary mesenchyme directs lung development. *Curr Opin Genet Dev* 32:98–105.
32. Rankin SA, Zorn AM (2014) Gene regulatory networks governing lung specification. *J Cell Biochem* 115:1343–1350.
33. Koshiba-Takeuchi K, et al. (2009) Reptilian heart development and the molecular basis of cardiac chamber evolution. *Nature* 461:95–98, and erratum (2009) 461:550.
34. Rankin SA, et al. (2015) A molecular atlas of Xenopus respiratory system development. *Dev Dyn* 244:69–85.
35. Brown DD, et al. (2005) Tbx5 and Tbx20 act synergistically to control vertebrate heart morphogenesis. *Development* 132:553–563.
36. Goetz SC, Brown DD, Conlon FL (2006) TBX5 is required for embryonic cardiac cell cycle progression. *Development* 133:2575–2584.
37. Kimura S, et al. (1996) The T/ebp null mouse: Thyroid-specific enhancer-binding protein is essential for the organogenesis of the thyroid, lung, ventral forebrain, and pituitary. *Genes Dev* 10:60–69.
38. Poulain M, Ober EA (2011) Interplay between Wnt2 and Wnt2bb controls multiple steps of early foregut-derived organ development. *Development* 138:3557–3568.
39. Winata CL, et al. (2009) Development of zebrafish swimbladder: The requirement of hedgehog signaling in specification and organization of the three tissue layers. *Dev Biol* 331:222–236.
40. Yin A, Korzh S, Winata CL, Korzh V, Gong Z (2011) Wnt signaling is required for early development of zebrafish swimbladder. *PLoS One* 6:e18431.
41. Cass AN, Servetnick MD, McCune AR (2013) Expression of a lung developmental cassette in the adult and developing zebrafish swimbladder. *Evol Dev* 15:119–132.
42. Zheng W, et al. (2011) Comparative transcriptome analyses indicate molecular homology of zebrafish swimbladder and mammalian lung. *PLoS One* 6:e24019.
43. Tatsumi N, et al. (2016) Molecular developmental mechanism in polypterid fish provides insight into the origin of vertebrate lungs. *Sci Rep* 6:30580.
44. Longo S, Riccio M, McCune AR (2013) Homology of lungs and gas bladders: Insights from arterial vasculature. *J Morphol* 274:687–703.
45. Garrity DM, Childs S, Fishman MC (2002) The heartstrings mutation in zebrafish causes heart/fin Tbx5 deficiency syndrome. *Development* 129:4635–4645.
46. Ng JK, et al. (2002) The limb identity gene Tbx5 promotes limb initiation by interacting with Wnt2b and Fgf10. *Development* 129:5161–5170.
47. Ahn DG, Kourakis MJ, Rohde LA, Silver LM, Ho RK (2002) T-box gene tbx5 is essential for formation of the pectoral limb bud. *Nature* 417:754–758.
48. Parrie LE, Renfrew EM, Wal AV, Mueller RL, Garrity DM (2013) Zebrafish tbx5 paralogs demonstrate independent essential requirements in cardiac and pectoral fin development. *Dev Dyn* 242:485–502.
49. Zhou L, et al. (2015) Tbx5 and Osr1 interact to regulate posterior second heart field cell cycle progression for cardiac septation. *J Mol Cell Cardiol* 85:1–12.
50. Bellusci S, et al. (1997) Involvement of sonic hedgehog (Shh) in mouse embryonic lung growth and morphogenesis. *Development* 124:53–63.
51. Pepicelli CV, Lewis PM, McMahon AP (1998) Sonic hedgehog regulates branching morphogenesis in the mammalian lung. *Curr Biol* 8:1083–1086.
52. Peyrot SM, Wallingford JB, Harland RM (2011) A revised model of Xenopus dorsal midline development: Differential and separable requirements for notch and Shh signaling. *Dev Biol* 352:254–266.
53. Bowes JB, et al. (2010) Xenbase: Gene expression and improved integration. *Nucleic Acids Res* 38:D607–D612.
54. James-Zorn C, et al. (2018) Navigating Xenbase: An integrated Xenopus genomics and gene expression database. *Methods Mol Biol* 1757:251–305.
55. Karpinka JB, et al. (2015) Xenbase, the Xenopus model organism database; new virtualized system, data types and genomes. *Nucleic Acids Res* 43:D756–D763.
56. Chen JK, Taipale J, Cooper MK, Beachy PA (2002) Inhibition of hedgehog signaling by direct binding of cyclopamine to smoothened. *Genes Dev* 16:2743–2748.
57. Wu X, Ding S, Ding Q, Gray NS, Schultz PG (2002) A small molecule with osteogenesis-inducing activity in multipotent mesenchymal progenitor cells. *J Am Chem Soc* 124: 14520–14521.
58. Buenrostro JD, Wu B, Chang HY, Greenleaf WJ (2015) ATAC-seq: A method for assaying chromatin accessibility genome-wide. *Curr Protoc Mol Biol* 109:21.29.1–21.29.9.
59. He A, Kong SW, Ma Q, Pu WT (2011) Co-occupancy by multiple cardiac transcription factors identifies transcriptional enhancers active in heart. *Proc Natl Acad Sci USA* 108: 5632–5637.
60. Luna-Zurita L, et al. (2016) Complex interdependence regulates heterotypic transcription factor distribution and coordinates cardiogenesis. *Cell* 164:999–1014.
61. Nadadur RD, et al. (2016) Pitx2 modulates a Tbx5-dependent gene regulatory network to maintain atrial rhythm. *Sci Transl Med* 8:354ra115.
62. Jolma A, et al. (2013) DNA-binding specificities of human transcription factors. *Cell* 152:327–339.
63. Arnolds DE, et al. (2012) TBX5 drives Scn5a expression to regulate cardiac conduction system function. *J Clin Invest* 122:2509–2518.
64. Smemo S, et al. (2012) Regulatory variation in a TBX5 enhancer leads to isolated congenital heart disease. *Hum Mol Genet* 21:3255–3263.
65. Iacovino M, et al. (2011) Inducible cassette exchange: A rapid and efficient system enabling conditional gene expression in embryonic stem and primary cells. *Stem Cells* 29:1580–1588.
66. Kattman SJ, et al. (2011) Stage-specific optimization of activin/nodal and BMP signaling promotes cardiac differentiation of mouse and human pluripotent stem cell lines. *Cell Stem Cell* 8:228–240.
67. Trujillo GV, et al. (2016) The canonical Wingless signaling pathway is required but not sufficient for inflow tract formation in the Drosophila melanogaster heart. *Dev Biol* 413:16–25.
68. Agarwal P, et al. (2003) Tbx5 is essential for forelimb bud initiation following patterning of the limb field in the mouse embryo. *Development* 130:623–633.
69. Rallis C, et al. (2003) Tbx5 is required for forelimb bud formation and continued outgrowth. *Development* 130:2741–2751.
70. Horb ME, Thomsen GH (1999) Tbx5 is essential for heart development. *Development* 126:1739–1751.
71. Tseng YR, et al. (2007) Holt-Oram syndrome with right lung agenesis caused by a de novo mutation in the TBX5 gene. *Am J Med Genet A* 143A:1012–1014.
72. Qin X, Wei W, Fangqi G (2015) Horseshoe lung associated with Holt-Oram syndrome. *Iran J Pediatr* 25:e251.
73. de Jong EM, Felix JF, de Klein A, Tibboel D (2010) Etiology of esophageal atresia and tracheoesophageal fistula: "Mind the gap". *Curr Gastroenterol Rep* 12:215–222.
74. Wain LV, et al.; UK Brain Expression Consortium (UKBEC); OxGSK Consortium (2015) Novel insights into the genetics of smoking behaviour, lung function, and chronic obstructive pulmonary disease (UK BiLEVE): A genetic association study in UK Biobank. *Lancet Respir Med* 3:769–781.
75. Zhu Y, et al. (2008) Tbx5-dependent pathway regulating diastolic function in congenital heart disease. *Proc Natl Acad Sci USA* 105:5519–5524.
76. Lewis ZR, Hanken J (2017) Convergent evolutionary reduction of atrial septation in lungless salamanders. *J Anat* 230:16–29.
77. St-Jacques B, et al. (1998) Sonic hedgehog signaling is essential for hair development. *Curr Biol* 8:1058–1068.
78. Zhang XM, Ramalho-Santos M, McMahon AP (2001) Smoothened mutants reveal redundant roles for Shh and Ihh signaling including regulation of L/R symmetry by the mouse node. *Cell* 106:781–792.
79. Sive HL, Grainger RM, Harland RM (2000) *Early Development of Xenopus laevis: A Laboratory Manual* (Cold Spring Harbor Lab Press, Cold Spring Harbor, NY), p ix, 338 p.
80. Tandon P, Showell C, Christine K, Conlon FL (2012) Morpholino injection in Xenopus. *Methods Mol Biol* 843:29–46.
81. Westerfield M (2007) *The Zebrafish Book* (Univ Oregon Press, Eugene, OR), 5th Ed.
82. Nasevicius A, Ekker SC (2000) Effective targeted gene 'knockdown' in zebrafish. *Nat Genet* 26:216–220.
83. Wilkinson DG, Nieto MA (1993) Detection of messenger RNA by in situ hybridization to tissue sections and whole mounts. *Methods Enzymol* 225:361–373.
84. Takada S, et al. (1994) Wnt-3a regulates somite and tailbud formation in the mouse embryo. *Genes Dev* 8:174–189.
85. Jensen B, et al. (2012) Identifying the evolutionary building blocks of the cardiac conduction system. *PLoS One* 7:e44231.
86. Jensen B, et al. (2018) Specialized impulse conduction pathway in the alligator heart. *eLife* 7:e32120.
87. Poelmann RE, et al. (2014) Evolution and development of ventricular septation in the amniote heart. *PLoS One* 9:e106569.
88. Langmead B, Salzberg SL (2012) Fast gapped-read alignment with Bowtie 2. *Nat Methods* 9:357–359.
89. Zhang Y, et al. (2008) Model-based analysis of ChIP-seq (MACS). *Genome Biol* 9:R137.
90. Feng J, Liu T, Qin B, Zhang Y, Liu XS (2012) Identifying ChIP-seq enrichment using MACS. *Nat Protoc* 7:1728–1740.